

# The watercolor illusion and neon color spreading: a unified analysis of new cases and neural mechanisms

Baingio Pinna

*Facoltà di Lingue e Letterature Straniere, Università di Sassari, via Roma 151, I-07100, Sassari, Italy*

Stephen Grossberg

*Department of Cognitive and Neural Systems and Center for Adaptive Systems, Boston University,  
677 Beacon Street, Boston, Massachusetts 02215*

Received January 18, 2005; accepted April 14, 2005

Coloration and figural properties of neon color spreading and the watercolor illusion are studied using phenomenal and psychophysical observations. Coloration properties of both effects can be reduced to a common limiting condition, a nearby color transition called the two-dot limiting case, which clarifies their perceptual similarities and dissimilarities. The results are explained by the FACADE neural model of biological vision. The model proposes how local properties of color transitions activate spatial competition among nearby perceptual boundaries, with boundaries of lower-contrast edges weakened by competition more than boundaries of higher-contrast edges. This asymmetry induces spreading of more color across these boundaries than conversely. The model also predicts how depth and figure-ground effects are generated in these illusions. © 2005 Optical Society of America

*OCIS codes:* 330.0330, 330.1720, 330.4060, 330.4270, 330.5020, 330.5510, 330.7310.

## 1. INTRODUCTION: A CURRENT VIEW OF A SEMINAL DISCOVERY OF DEVALOIS

Russell DeValois and his colleagues discovered many seminal neurobiological data that have been influential in developing concepts about how the visual cortex sees. The Thorell *et al.*<sup>1</sup> study helped to inspire and support modeling concepts that were developed at around the same time. This important article reported data from macaque monkey that showed that “simple cells ... are distinguished by relatively narrow color specificity” (p. 761). In contrast, “complex color cells ... responded uniformly to many (or, in the extreme, all) equiluminant wavelength changes .... The RFs of many of these cells (15/31, 48%) were composed of overlapping color-regions” (p. 762), and “these cells always responded with the same polarity to all colors tested. This was in keeping with one of the criterial features of complex cell behavior: their lack of phase specificity” (p. 764). Thorell *et al.*<sup>1</sup> went on to conclude that these complex cells “must surely be considered color cells in the broadest sense. They clearly use color information to detect the presence of spatial patterns” (p. 768).

At around this time, Cohen and Grossberg<sup>2</sup> and Grossberg and Mingolla<sup>3,4</sup> were introducing their concepts that the visual cortex computes perceptual boundaries and surfaces in parallel processing streams. This conclusion was derived primarily from a perceptual analysis, so Grossberg and his colleagues searched for neurobiological evidence to confirm or deny that this actually happens.

One timely piece of evidence was the Thorell *et al.*<sup>1</sup> study, which supported the early prediction that these boundaries and surfaces are processed by the interblob and blob streams, respectively, from V1 to V4. It should be emphasized that the prediction of parallel boundary and surface streams differs in significant, indeed profound, ways from the prediction that parallel cortical streams compute orientations and colors. Within the boundary/surface conception, complex cells in V1 pool over opposite polarities and colors as part of the process of computing good boundary signals. Because of this pooling, however, the prediction was made that “all boundaries are invisible,” or amodal, within the boundary stream. This conclusion followed from the fact that, because boundaries pool over opposite luminance polarities and colors, they cannot represent the difference between light and dark or between different colors. Grossberg and his colleagues thus concluded that the property that Thorell *et al.*<sup>1</sup> reported about “color cells in the broadest sense” was exactly what was needed to build good boundary signals. However, Grossberg and colleagues also predicted that the activities of these boundary cells were, in themselves, invisible or amodal and therefore did not carry a visible color signal. Visible colors were predicted to be represented within the surface stream, whose interactions with the boundary stream define the regions within which visible surface lightnesses and colors are restricted. The present article shows how this insight can be used to provide a unifying explanation of recent data about neon color spreading and the water-

color illusion, two classes of phenomena that enable visible colors of the surface stream to be dissociated from figural properties that are initiated in the boundary stream.

## 2. NEON COLOR SPREADING

Varin<sup>5</sup> studied a “chromatic spreading” effect induced when four sets of concentric black circumferences are arranged in a crosslike shape and are partially composed of blue arcs that create a virtual large central blue circle (see Fig. 1(a)). The central virtual circle appears as a ghostly transparent veil or as a chromatic translucent diffusion of bluish tint spreading among the boundaries of the blue arcs. The chromatic spreading fills the whole illusory circle induced by the terminations of the black arcs (see Bressan *et al.*<sup>6</sup> for a review).

The neon effect was independently reported in 1975 by van Tuijl<sup>7</sup> (see also van Tuijl and de Weert<sup>8</sup>), who named it “neon-like color spreading.” Van Tuijl used a lattice of horizontal and vertical black lines, where segments creating an inset virtual diamond shape had a different color (e.g., blue). The perceptual result is a delicately tinted transparent diamondlike veil above the lattice (see Fig. 1(b)). The common geometrical property of the known cases of neon color spreading is the continuation of one line in a second line differently colored or, otherwise stated, a single continuous line varying at a certain point from one color to another. Neon color spreading manifests two basic phenomenal properties: coloration and figural effects, which are discussed below.

### A. Coloration Effects in Neon Color Spreading

The phenomenology of the coloration effect within neon color spreading points out the following properties, mostly depending on the luminance contrast between the two inducing lines. (i) The color is perceived as a diffusion of a certain quantity of pigment of the inset chromatic segments. (ii) The appearance of the spreading color (*Erscheinungsweise*, Katz<sup>9,10</sup>) is diaphanous and glows like a smoggy neon on the background or (most under achromatic conditions) like a shadowy, foggy, dirty, or filmy

transparent veil. (iii) When the inset virtual figure is achromatic and the surrounding inducing elements are chromatic, the illusory veil appears tinted not in the achromatic color of the embedded elements, as expected, but in the complementary color of the surrounding elements; for example, the achromatic components appear to spread reddish or yellowish color when the surrounding components are, respectively, green or blue.<sup>7</sup>

### B. Figural Effects in Neon Color Spreading

The previous coloration qualities are strongly linked to the figural effects of neon color spreading. Phenomenally, (i) the illusory neon region has a depth stratification: It typically appears in front of the component elements; (ii) the illusory region is perceived as a transparent film; (iii) by reversing the relative contrast of inset versus surrounding components, the depth stratification reverses as well; for example, when the surrounding elements have less contrast than the inset ones, as illustrated in Fig. 2, the inset components appear as a background rather than as a foreground;<sup>11</sup> (iv) the illusory region may assume different figural roles or may become different objects; for example, a “light,” a “veil,” a “shadow,” or a “fog”; (v) neon color spreading illustrates a “phenomenal scission” (*Spaltung*, Koffka;<sup>12</sup> Metzger<sup>13</sup>) of an elevated transparent colored veil and underneath components that appear to amodally continue without changing in color.

## 3. WATERCOLOR ILLUSION

The “watercolor illusion” is a long-range spread of color (up to 45° visual angle) diffusing from a thin colored line running parallel and contiguous to a darker chromatic contour and imparting a strong figural effect across large regions;<sup>14–19</sup> also see von Campenhausen and Schramme<sup>20</sup> for a discussion of Fechner–Benham subjective color, which can also spread to around 40°. In Fig. 3, purple undulating contours flanked by orange edges are perceived as undefined irregular curved shapes evenly colored by a light veil of orange tint spreading from the

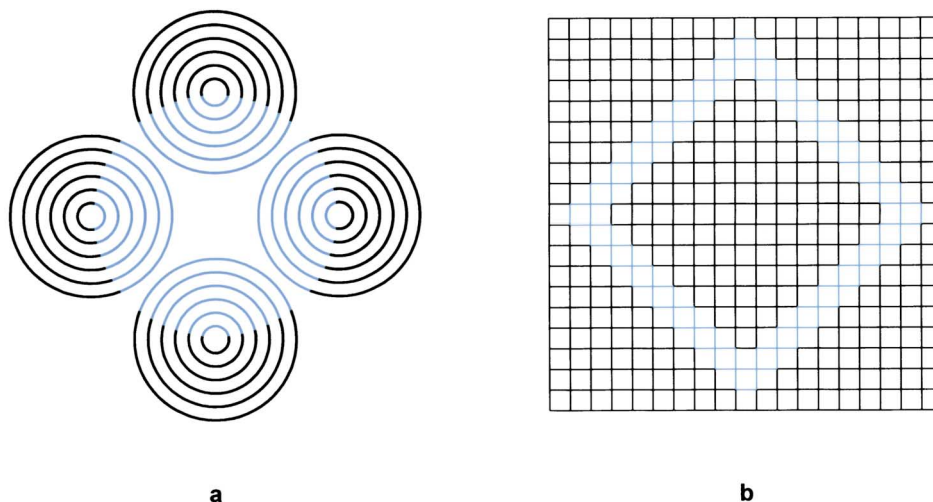


Fig. 1. Neon color spreading: a, The central virtual circle and b, the inset virtual diamond shape appear as a ghostly overlapping transparent veil of bluish tint spreading among the boundaries of the blue components.

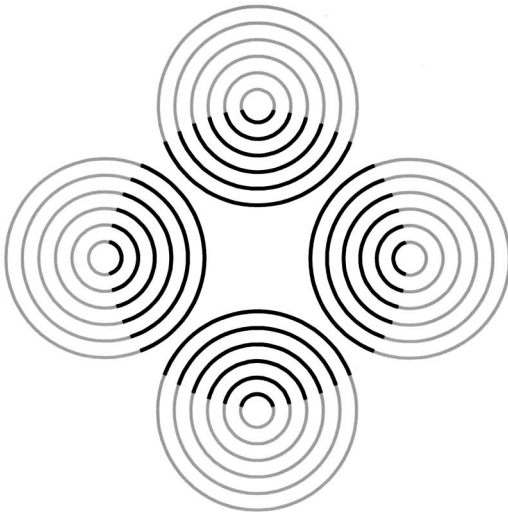


Fig. 2. Figural effect of the neon color spreading: When the surrounding elements have less contrast than the inset ones, the inset components appear as a background rather than as a foreground.

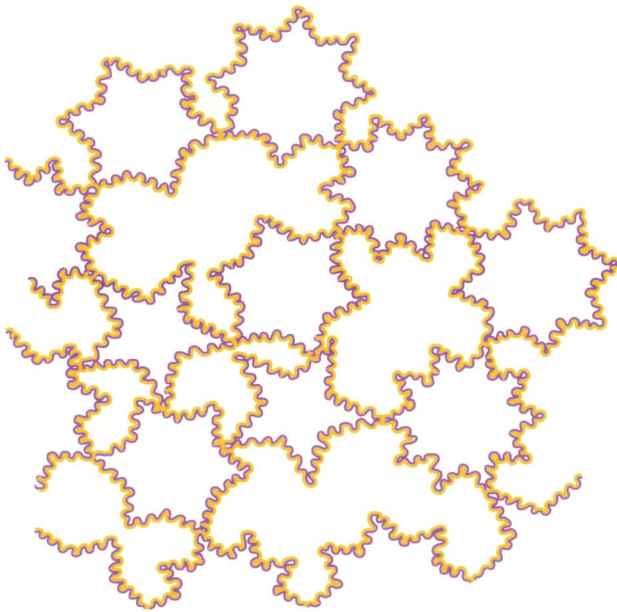


Fig. 3. Watercolor illusion: purple undulated contours flanked by orange edges are perceived as undefined irregular curved shapes with a plain volumetric effect evenly colored by a light veil of orange tint spreading from the orange edges.

orange edges. All the chromatic combinations of the two lines produce similar effects (see Pinna<sup>15</sup> and Pinna *et al.*<sup>16</sup>).

In Fig. 4, stars with a varying number of points are now perceived evenly colored of the same illusory faint orange as in Fig. 3. The different results of Figs. 3 and 4, although both figures have the same geometrical structure, depend on the inversion of the purple and orange lines: The purple/orange line arrangement of Fig. 3 becomes the orange/purple of Fig. 4. This reversion affects both the coloration and the figural effects of the watercolor illusion: What in Fig. 3 appears as illusory tinted and segregated as a figure, in Fig. 4 appears as an empty space without a clear coloration.

Geometrically, whereas neon color spreading is elicited by a single continuous line changing one color into another, the watercolor illusion occurs through the juxtaposition of at least two differently colored parallel lines.

#### A. Coloration Effects in the Watercolor Illusion

The phenomenology of the coloration effect within the watercolor illusion highlights some properties that appear analogous to and some different from those of neon color spreading: (i) As in neon color spreading, the illusory color is perceived as a spreading of some quantity of tint belonging to the orange line and giving rise to a more diluted orange (yellow) coloration; (ii) the coloration does not appear transparent as in neon color spreading but opaque and belonging to a solid impenetrable object; (iii) the coloration appears epiphanous and as a surface color;<sup>10</sup> (iv) like neon color spreading, the watercolor illusion produces a complementary color when one of the two juxtaposed lines is achromatic and the other chromatic.<sup>21</sup>

#### B. Figural Effects in the Watercolor Illusion

Besides the coloration effect, the watercolor illusion determines a unique figural effect that competes with the classical Gestalt principles of grouping and figure-ground segregation.<sup>22-24</sup> All else being equal, Pinna *et al.*<sup>16</sup> and Pinna<sup>19</sup> demonstrated that the watercolor illusion determines figure-ground segregation more strongly than the Gestalt principles of proximity, good continuation, prägnanz, closure, symmetry, convexity, past experience, and similarity. It was also shown in Pinna<sup>19</sup> that the watercolor illusion includes a new principle of figure-ground segregation, the asymmetric luminance contrast principle, stating that, all else being equal, given an asymmetric luminance contrast on both sides of a boundary, the region whose luminance gradient is less abrupt is perceived as a figure relative to the complementary more abrupt region, which is perceived as a background. This

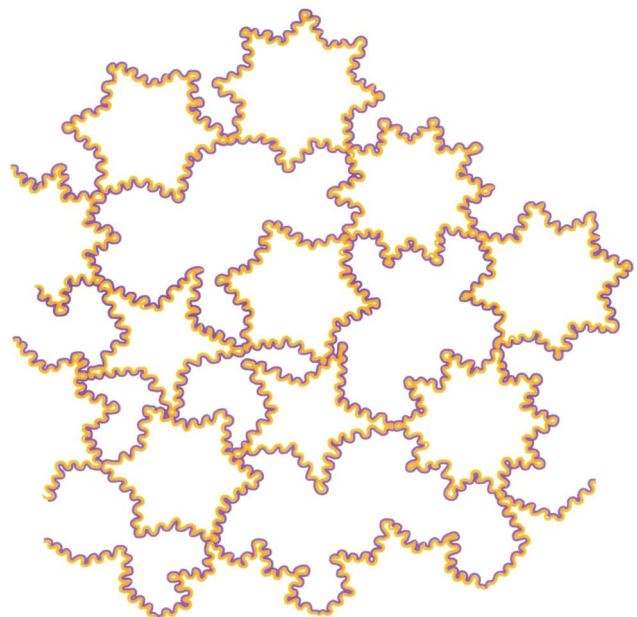


Fig. 4. When purple and orange lines in Fig. 3 are reversed, stars with a different number of points are now perceived.

phenomenal and physical asymmetry across the boundaries makes the figural effect due to the watercolor illusion stronger than in classical figure-ground conditions and prevents reversibility of figure-ground segregation. The asymmetric luminance contrast principle strengthens Rubin's principle of unilateral belongingness of boundaries<sup>23</sup>: The boundaries belong only to the figure and not to the background, which appears as an empty space without a defined shape.

The main figural qualities of the watercolor illusion are as follows: (i) The illusory figure has a univocal (poorly reversible) depth segregation similar to a rounded surface with a bulging and volumetric effect (ii) The resulting surface appears thick, solid, opaque, and dense (iii) As shown in Figs. 3 and 4, by reversing the colors of the two parallel lines, figure-ground segregation reverses as well; in these two figures, the border ownership is also reversed: the boundaries belong only to one region and not to the other. (iv) As in neon color spreading, the figural effect of the watercolor illusion may be perceived in terms of phenomenal scission but with a different mode of appearance; that is, as a figure showing a strong depth segregation and appearing as a volumetric rounded object within a three-dimensional (3D) space, while the perceived variation of color, going from the boundaries to the center of the object, may be seen as a gradient of shading, as if light were reflected onto a volumetric and rounded object, so that the variation of color appears to be the homogeneous color of the object. Object and light are the two split emergent components of the scission.

Summing up, neon color spreading differs from the watercolor illusion both in the appearance of the coloration (respectively, transparent versus solid and impenetrable, and diaphanous versus epiphanous) and in the figural effects (respectively, transparent versus opaque and dense appearance, and appearance as a "light," a "veil," a "shadow," or a "fog" versus rounded thick and opaque surface bulging from the background).

#### 4. NEON COLOR SPREADING AND WATERCOLOR ILLUSION: SIMILARITIES AND DIFFERENCES

Despite the specific differences, the two illusions are phenomenally similar in their strong color spreading and clear depth segregation. We suggest that, while the similarities may be attributed to the local nearby transition of colors that are common to both illusions, the differences may be attributed to the global geometrical boundary conditions that differ in the two illusions, notably, the continuation of a segment of a different color in neon color spreading and the juxtaposition of at least two lines in the watercolor illusion.

If this is true, then the differences between the two illusions can be reduced under modified geometrical conditions, and, by reaching a limiting case, they can be eliminated. The questions to answer in this section are thus: Can the watercolor illusion assume coloration and figural properties similar to those of neon color spreading? Can the two illusions be reduced to a simple limiting case based on local nearby transitions of colors where coloration and figural effects are still perceived?

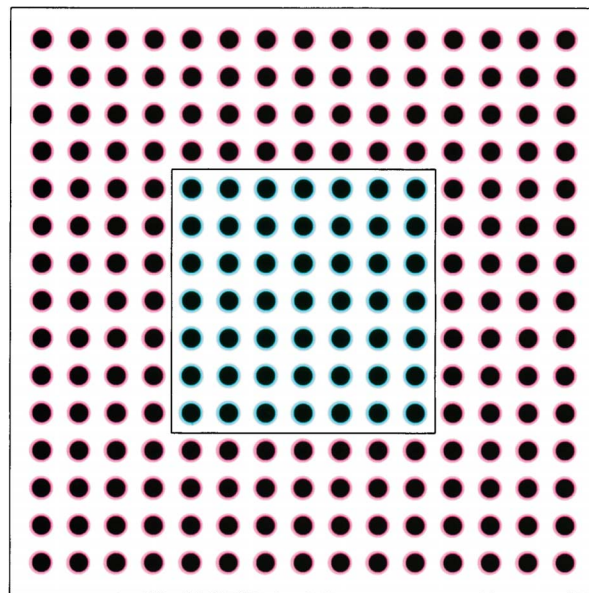


Fig. 5. Light blue coloration spreading from the inset square of elements appears surrounded by a red spreading. The coloration effect is not accompanied by a figural effect with a plain volumetric property, but it appears diaphanous like a foggy veil of color.

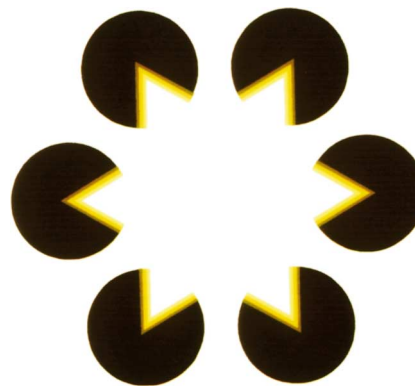


Fig. 6. Illusory coloration of the star appears fuzzy and luminous and manifests a poor surface appearance.

##### A. Coloration and Figural Variations of the Watercolor Illusion and Neon Color Spreading

By increasing the width of one of the two juxtaposed lines of the watercolor illusion to such an extent that the line becomes a surface, the watercolor illusion manifests different coloration and figural effects. Under these conditions, the surface may be segregated independently from the colored fringes. The resulting coloration does not assume surface color properties but properties belonging to the background: It is perceived diaphanous like a foggy coloration diffusing everywhere in the background or as a colored light (see Fig. 5).

In Fig. 6, the coloration effect gives to the illusory star a fuzzy luminous quality. Whereas in Fig. 5 the coloration belongs to the background, in Fig. 6 it is a property belonging to the figure; however, the star does not manifest the strong surface appearance peculiar to Figs. 3 and 4: Its inner surface appears brighter and yellowish, foggy and smooth.

A fuzzy surface coloration, but with a more volumetric

figural effect, is illustrated in Fig. 7. The columns bulge in depth even if they appear softly and nebulously colored.

In Fig. 8, the watercolored frame appears transparent, as in neon color spreading.

In Fig. 9, a comparison between quasi-equiluminant conditions and high-contrast differences between the two juxtaposed color lines induces different coloration and figural effects: Around the quasi-equiluminant conditions, the coloration appears not as a surface color but as an ethereal soft coloration without clear figural or background properties; around the high-contrast differences, the figural effect and the surface color properties are restored.

Taken together, these figures suggest that in the watercolor illusion: (i) the modes of appearance of coloration are strongly related to boundary conditions that induce specific figural effects; (ii) by changing the boundary conditions, coloration and figural properties are seen that are analogous to those of neon color spreading; (iii) given this variety of appearances on the basis of different conditions, a simpler set of boundary conditions, or a limiting case, can unify both effects using local transitions of colors and can help to explain similarities and dissimilarities of the two illusions.

### B. Toward a Limiting Case

Figure 10(a) shows a case of neon color spreading where purple surrounding arcs continue in orange arcs. The inset square annulus appears not to glow, as in Fig. 1, but is rather perceived as a transparent orange veil. This difference in appearance of both coloration and figural effects is possibly due to the high contrast between the two colors relative to each other.

Because neon color spreading and the watercolor illusion are, respectively, defined by the continuation and juxtaposition of lines, the two illusions can be gradually combined, as illustrated in Figs. 10(b) and 10(c), and reduced to the limiting case in Fig. 10(d). Geometrically, in

Fig. 10(b), the orange inset arcs are reduced to short dashes, creating a condition in between neon color spreading and the watercolor illusion: From the neon-color-spreading point of view, the inducing elements are lines that continue in short dashes, but, from the watercolor point of view, the termination of each inducing arc has a juxtaposed short dash. A clear coloration effect is perceived, not weaker than that of Fig. 10(a), but it has a diaphanous and poor surface appearance and a figural effect describable as a fuzzy illusory square annulus that is yellowish and brighter than the background. This phenomenal result is similar to that of Figs. 5 and 6. Note that the reduction of dashes to dots with the same diameter as the width of the purple arcs or even smaller does not change the strength of these effects.

The opposite geometrical condition, once again in between neon color spreading and the watercolor illusion, is illustrated in Fig. 10(c). Here, the purple surrounding arcs of Fig. 10(a) are reduced to short dashes. Under these conditions, a coloration effect weaker than that of Fig. 10(a) is perceived.

The percepts of Figs. 10(b) and 10(c) suggest that local nearby transitions of colors may be responsible for the coloration and figural effects in both illusions, even if the coloration and figural effects change their mode of appearance (Fig. 10(b)) or their strength (Fig. 10(c)). If this is true, then by reducing both purple and orange arcs to short dashes, the coloration and figural effects should be still perceived (see Fig. 10(d)). By reducing the dashes to dots, the strength of these effects does not change. It has been already shown that the watercolor illusion occurs not only by using juxtaposed lines but also by using juxtaposed chains of dots (see Pinna *et al.*<sup>16</sup>). Under these conditions both coloration and figural effects become weaker as the density of the dots becomes sparser.

We suggest that the two-dot juxtaposition may represent a limiting case for neon color spreading and the watercolor illusion. More specifically, (i) the two-dot limiting

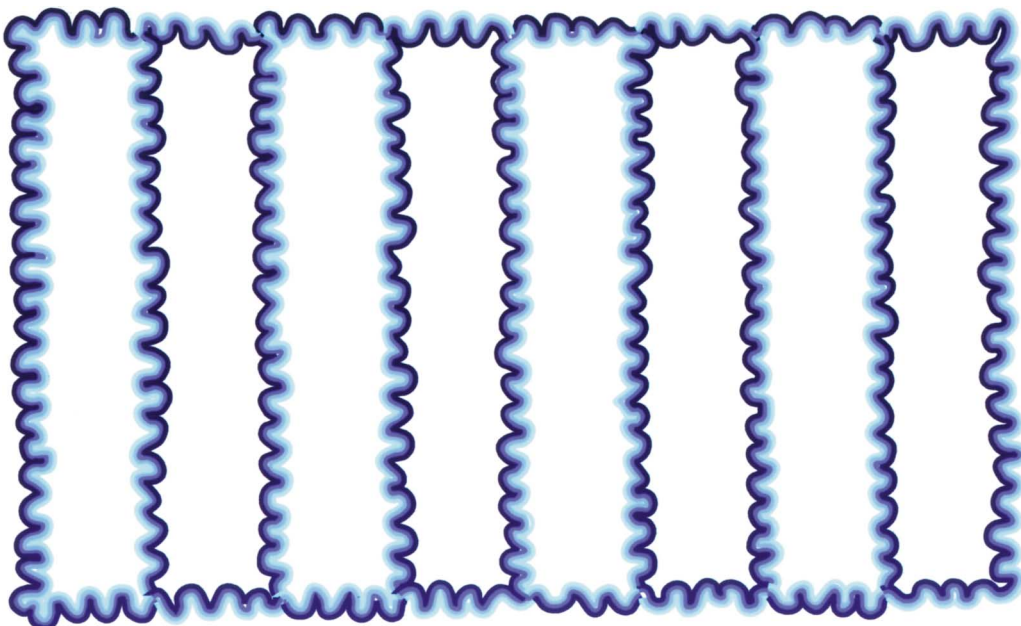


Fig. 7. columns bulge in the 3D space even if they appear softly and nebulously colored.

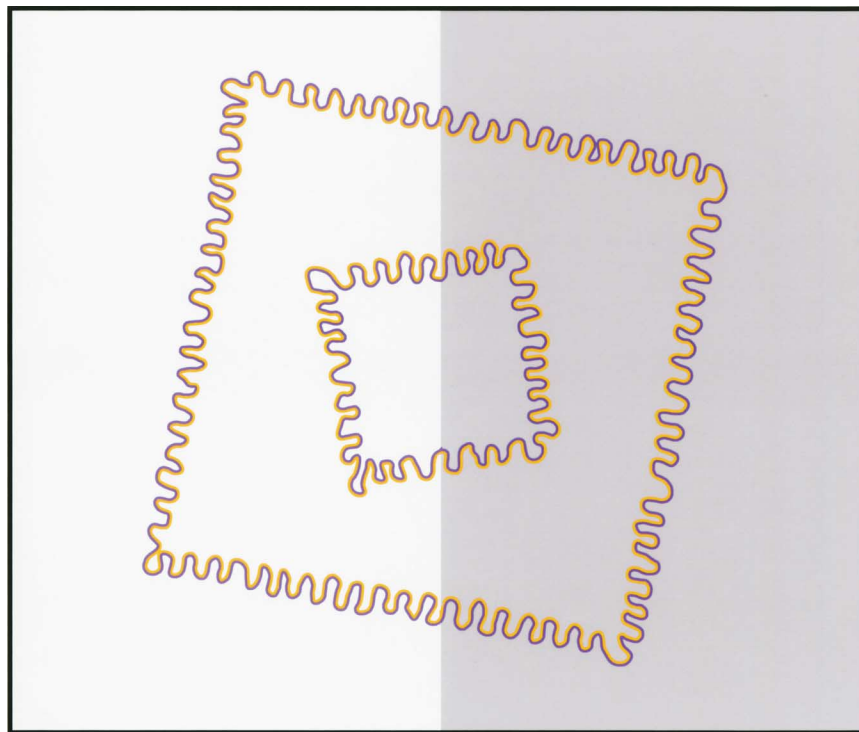


Fig. 8. A transparent watercolored frame.

case can be considered the phenomenal basis for the coloration and figural effects in both illusions. (ii) Given these basic conditions, the specific mode of appearance of coloration and figural effects in the two illusions may be elicited by different local and global distributions of nearby transitions of colors that create different boundary organizations. (iii) This limiting case has the advantage of providing support for a simple common neural model (see Section 6). Coloration and figural effects may derive from parallel processes: At a feature processing stage, the small interaction area around and between the two dots produces the color spreading common to both illusions, and, at a parallel boundary processing stage, the different geometrical structures in both illusions organize the color spreading to generate different figural effects.

Despite these advantages, Figs. 10(b)–10(d) raise two sorts of issues. On the one hand, the geometrical reduction causes changes in both the strength and the mode of appearance of the coloration and figural effects. A systematic measurement is needed to evaluate how the strength of coloration changes by progressively reducing the length of the inducing purple arcs. This is the topic of the experiment in Section 5. As regards the modes of appearance of the coloration and figural effects, small variations suffice to induce large qualitative effects that are difficult to quantify and predict, as shown in Figs. 3–9 for the watercolor illusion.

On the other hand, to appropriately assume the two-dot juxtaposition as a limiting case, the strength of its color spreading has to be compared with that induced by other phenomena related to neon color spreading, such as the chromatic assimilation of the inner orange arcs of Fig. 10(a) when the purple surrounding arcs are removed.<sup>11,25,26</sup> Under these conditions, the white space

in between the arcs of the square annulus appears orange-ish, as if the white regions assimilate the color of the arcs. A comparison between the two kinds of color spreading is needed to show that the coloration induced by the two-dot limiting case has a different nature compared with that of the assimilation phenomenon. This comparison is also the topic of the next experiment.

## 5. EXPERIMENT: NEON COLOR SPREADING AND WATERCOLOR ILLUSION COMBINED IN A NEW LIMITING CASE

Bressan<sup>11,26</sup> proposed that assimilation and neon spreading may obey the same basic diffusion mechanism in inducing the coloration effect and that the difference between the two effects is the phenomenal scission of the coloration from the plane of the figure in the form of a transparent layer. Assimilation does not create this kind of scission. The best perceptual condition for obtaining the phenomenal scission is the inset of colored drawings (e.g., orange arcs creating the square annulus of Fig. 10(a)) in the blank area in continuation with the outer drawing (e.g., purple arcs of Fig. 10(a)) that would otherwise produce a strong illusory figure.<sup>6,26</sup>

The questions to be answered in this experiment are: Given the watercolor illusion and more specifically the two-dot limiting case, can chromatic assimilation still be considered a basic effect for neon color spreading? Is the illusory figure and, as a consequence, the transparent phenomenal scission really needed to cause neon color spreading? Is the strength of the coloration effect due to the two-dot limiting case sufficient to explain the coloration of neon color spreading and of the watercolor illusion?

As illustrated in Figs. 10(b) and 10(d), our hypothesis is that assimilation may not be needed to induce the coloration effect of neon color spreading, and, owing to incomparable geometric constructions among the three illusions, assimilation cannot be considered a basic effect for either neon color spreading or the watercolor illusion. A common element based on nearby transitions of colors is structurally preferable. However, assimilation may play a role in neon color spreading but not necessarily in summing up its coloration effect to the one induced by the limiting case. The experimental results can clarify this point.

Furthermore, illusory contours do not necessarily play any role in neon color induction. In fact, as illustrated in Fig. 10(b), after the inner orange arcs are removed, the small dashes do not produce any illusory figure (apart from an emergent boundary that may contain the spread of color beyond the square annulus), even though they produce a plain coloration. In addition, the role of illusory contours is further weakened because the strength of the coloration of Fig. 10(b) is about as strong as the one of Fig. 10(a). Each small orange dash weakens illusory contour formation and brightness induction due to the purple arcs.<sup>27–29</sup> The fact that the coloration effect in Fig. 10(a) and 10(b) is approximately the same (see Fig. 11 below)

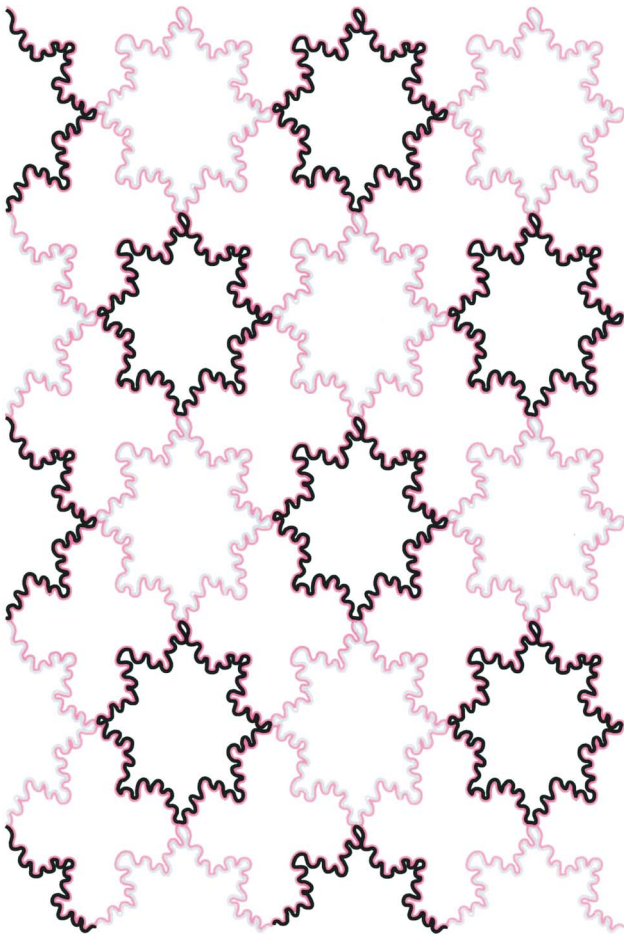


Fig. 9. Regions delimited by high-contrasted adjacent lines (black and red) show a clear figural effect and a surface color property, while the regions delimited by quasi-equiluminant adjacent lines (gray and red) show an ethereal soft coloration without any figural property.

but the illusory contours for the two cases have different strengths illustrates once again that coloration and figural effects are due to different processes.

Reducing both neon color spreading and the watercolor illusion to the two-dot limiting case, as illustrated in Fig. 10(d), suggests that coloration effects depend on nearby color transitions, whereas the figural differences between the two illusions may depend on how the global geometrical structure (e.g., size or length of each dot or line and their spatial arrangement) interacts with these color transitions to create context-sensitive perceptual differences.

### A. Subjects

Fifteen naïve subjects participated in the experiment. All observers had normal or corrected-to-normal vision.

### B. Stimuli

The stimuli were obtained by varying Fig. 10(a) in the following four conditions. (i) Three levels of length of purple arcs—not reduced to dashes as in Fig. 10(a), reduced to dashes of about 1.5 deg, and reduced to dashes of about 8.1 arc min; by varying the length of the purple arcs, the role of phenomenal scission, illusory contours, and assimilation is varied. (ii) Two levels of length of the orange arcs—not reduced to dashes, as in Fig. 10(a), and reduced to dashes of about 8.1 arc min; by changing the length of the orange arcs, the strength of the coloration due to the two-dot limiting case is tested. (iii) Assimilation of orange arcs obtained by removing the purple components of Fig. 10(a); under these conditions, the strength of the coloration due to the assimilation can be compared with that induced by neon color spreading and the watercolor illusion. (iv) Assimilation of short orange dashes obtained by removing the purple arcs when the orange arcs are reduced to the minimum length of 8.1 arc min; this is a control condition to evaluate if any coloration effect is perceived when only the orange components of the two-dot limiting case are shown.

The stroke width of the purple and orange arcs was approx 6.5 arc min. The CIE  $x, y$  chromaticity coordinates of the chromatic components of the patterns were (purple) 0.30, 0.23; (orange) 0.57, 0.42. Stimuli were presented on a white background and on a computer screen under Osram Daylight fluorescent light (250 lux, 5600 K). The overall size of the stimuli was about  $12.4 \times 12.4$  deg, the largest side of the square annulus was about 6.85 deg, and the width of the square annulus was about 1.15 deg.

### C. Procedure

Subjects viewed the stimuli with freely moving eyes using a chin-and-forehead rest positioned at 50 cm from the pattern. Magnitude estimation was used to quantify the perceived strength of the perceived coloration on an 8-point scale. The upper value 8 was defined by the coloration perceived in the inner edges of a square annulus created with wiggly purple and orange continuous contours and having about the same size of the square annulus of the stimuli, whereas the lower value 1 was defined by the complete absence of coloration obtained by removing the orange fringe from the upper modulus (see above the graph in Fig. 11). Subjects were allowed to exceed the up-

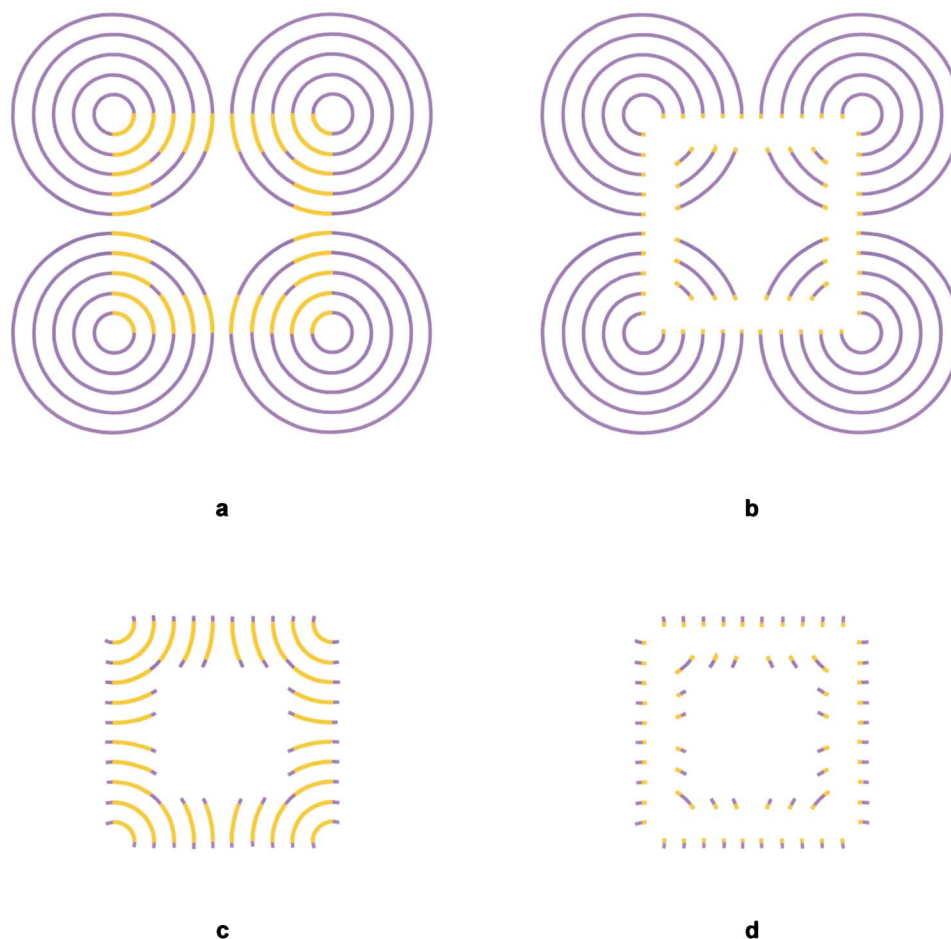


Fig. 10. Four conditions that gradually introduce a limiting case: (i) a, The neon color spreading defined by the continuation of lines of different color (a); (ii) b, a condition in between neon color spreading and watercolor illusion, where the orange inset arcs are reduced to short dashes (b); (iii) c, a condition once again in between neon color spreading and watercolor illusion, where the purple surrounding arcs of part “a” are reduced to short dashes; (iv) d, the two-dots limiting case obtained by reducing both purple and orange arcs to short dashes and considered as the basis for a common neural model to account for the neon color spreading and the watercolor illusion.

per modulus, in case one of the experimental stimuli should surpass the square annulus reference. The eight stimuli were presented consecutively to each observer in a random order.

There was a training period preceding each experiment to familiarize subjects with the color spreading in neon color spreading, the watercolor illusion, chromatic assimilation, and the task. During practice, subjects viewed some examples of neon color spreading, watercolor illusion, and assimilation different from the stimuli to familiarize them with these coloration effects. Observation time was unlimited.

#### D. Results and Discussion

Mean coloration ratings for each stimulus are plotted in Fig. 11. The results clearly showed that, by shortening the purple arcs when the orange arcs are not reduced (see stimuli 1, 2, and 3 in the abscissa of Fig. 11), the strength of the coloration effect decreases very little, less than 1 point of the magnitude scale ( $F2, 39=3.81, p<0.05$ ). This result confirms previous results reported by Redies and Spillmann<sup>25</sup> and Redies *et al.*<sup>30</sup>

In contrast, by shortening the purple arcs when the orange arcs are reduced to short dashes (see stimuli 4, 5,

and 6 in the abscissa of Fig. 11), the strength of the coloration effect increases within a small magnitude range scale of less than 1 point ( $F2, 39=3.49, p<0.05$ ). Significantly, no differences in the strength of the coloration were reported by the subjects between the two opposite conditions, the longest purple and orange arcs of stimulus 1 and the shortest purple and orange arcs of stimulus 6. This result clearly suggests the effectiveness of the two-dot limiting case as a good candidate to explain the coloration effects in neon color spreading. Furthermore, because the strength of the coloration in the watercolor illusion is directly proportional to the density of the dots (data not shown, see Pinna *et al.*<sup>16</sup>) and because a continuous line can be considered the highest density of dots, the gap of the coloration strength between stimulus 6 and the maximum coloration rating (see above the graph in Fig. 11) supports the effectiveness of the two-dot limiting case as a bridge even for the watercolor illusion.

Both assimilation conditions (iii, see stimulus 7 in the abscissa of Fig. 11) and (iv, see stimulus 8 in the abscissa of Fig. 11) confirm the basic role played by the two-dot limiting case. In fact, removing the purple components and therefore removing the nearby color transitions causes the strength of the coloration effect to abruptly

drop significantly (no statistics are needed) up to 2.7 in the assimilation of arcs (stimulus 7) and significantly (no statistics are needed) up to 1.1 in the assimilation of short dashes (stimulus 8), where the coloration is to be considered absent. These results suggest that even if orange arcs induce some coloration or chromatic assimilation, this effect is much weaker than (it does not sum up to) the coloration perceived in neon color spreading or in the limiting case and thus seems to be a different phenomenon.

The experimental results suggest that the coloration effect within neon color spreading and the watercolor illusion can be understood by considering the two-dot limiting case as the basis for a common neural mechanism useful to account for both illusions. However, the two illusions present many phenomenal dissimilarities, described in Sections 1–3 and not studied in the experiment, that may depend on the geometrical differences (continuation versus juxtaposition) eliciting singular local color interactions and figural organizations.

We suggest (see Section 6) that coloration and figural effects may derive from parallel processes, indeed from parallel cortical streams: At a feature processing or surface formation stream, the small interaction area around and between the two dots produces the color spreading common to both illusions; and at a parallel boundary pro-

cessing stream, the distinct geometrical structures present in both illusions produce the complex phenomenology of figural effects reported in Section 3. Color spreading may itself arise in two steps that involve an interaction between both the boundary and the surface streams (see Section 6). First, lateral inhibition can weaken the boundaries that surround the colored regions such that the weaker boundaries formed by smaller image contrasts are inhibited more, and second, color can spread through the weakened boundaries into the surrounding regions. Section 6 proposes how the FACADE neural model of 3D vision and figure-ground separation can more completely explain the experimental results as well as other properties of neon color spreading and the watercolor illusion.

### 6. FACADE NEURAL MODEL UNIFIES THE EXPLANATION OF NEON AND WATERCOLOR EFFECTS

#### A. Boundary Completion and Surface Filling-In

The distinct coloration and figural effects suggest that different mechanisms give rise to these properties. The proposed explanation below of these properties is given in a nontechnical way using a neural model of how the brain

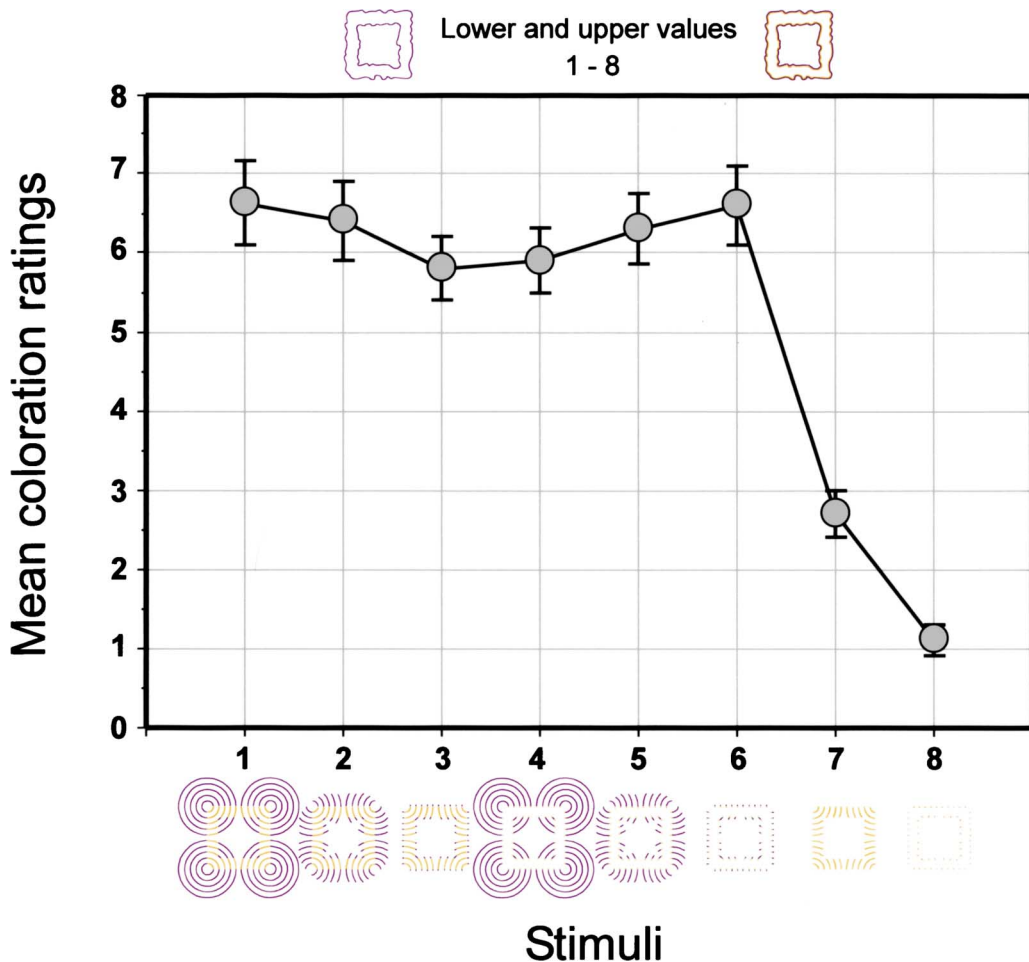


Fig. 11. Mean coloration ratings for four stimuli conditions: (i) Three levels of length of purple arcs; (ii) three levels of length of the orange arcs; (iii) chromatic assimilation of arcs obtained by removing purple components; (iv) assimilation of short orange dashes obtained by removing purple components. Above the graph, lower and upper values (1–8) used for the magnitude estimation are illustrated.

sees, which is called the FACADE model.<sup>31–33</sup> Many of the experimental manipulations that are described herein were developed to test predictions of the FACADE model, with positive results. FACADE model mechanisms have elsewhere been used to explain and predict perceptual, anatomical, and neurophysiological data different from those considered herein. These mechanisms have also been defined mathematically and verified using mathematical proofs or computer simulations. Background articles that contain such quantitative analyses are cited as part of the nontechnical summary below.

The FACADE model proposes how parallel boundary grouping and surface filling-in processes are carried out, respectively, by a boundary contour system (BCS) and a feature contour system (FCS).<sup>2–4,34,35</sup> These two processes are predicted to be realized by the cortical interblob and blob streams, respectively, within cortical areas V1 through V4. The boundary and surface processes exhibit complementary properties:<sup>36</sup> Boundaries form *inwardly* between similarly *oriented* contrasts and are *insensitive to contrast polarity* or, in other words, pool contrast information at each position from opposite contrast polarities. Boundaries pool opposite contrasts so that they can form around objects on textured backgrounds. In particular, a boundary can continuously surround an object even if its contrast relative to the background reverses multiple times as the object boundary is traversed. Because of this contrast-pooling property, all boundaries are predicted to be amodal within the interblob cortical stream wherein they form.

Visible colors and brightnesses, including neon color spreading and watercolor colorations, are predicted to be a property of the surface formation stream. Surfaces fill in *outwardly* from individual lightness or color inducers in an *unoriented* way using a process that is *sensitive to contrast polarity*. Surface filling-in is contained by boundaries, which act as barriers, or gates, that restrict the spread of color or brightness. This hypothesis implies that whenever surface colors are seen at locations far from their inducers they must have spread there via surface filling-in. Moreover, if surface color does manage to spread to positions beyond which they occur in a scene or image, then the boundaries that might otherwise have contained their spread must be broken or otherwise weakened to permit the leakage of color beyond them.

### B. Spatial Competition Weakens Boundaries in a Contrast-Sensitive Way

Typically, if a boundary is broken or weakened at a position where it might otherwise be expected to occur, this is due to some form of competition within the boundary system. Indeed, the BCS was, from the start,<sup>3,4,34</sup> predicted to include both spatial and orientational competition in order to explain a wide range of data about perceptual grouping and neon color spreading. From a deeper perspective, these competitive interactions may be viewed as a kind of hierarchical resolution of uncertainty whereby the brain compensates for deficiencies in boundary detection at line ends and corners that arise from the very existence of oriented receptive fields.

The main effect in the watercolor illusion, and more specifically the two-dot limiting case, can be explained by

interactions between three properties: boundary strength is contrast sensitive, nearby boundaries compete with each other via a process of spatial competition, and surface color can flow across positions where there are no boundaries or weak boundaries. As a result of contrast sensitivity, stronger boundaries tend to form in response to the edges of higher-contrast colored lines than at lower-contrast ones, so that stronger boundaries can inhibit nearby boundaries more than conversely, thereby enabling color to flow across these weakened boundaries. This interaction between boundary contrast, spatial competition, and boundary-gated surface filling-in provides an answer to the following questions: Why does a large luminance contrast difference between inducing lines show the strongest coloration effects? Why is there an asymmetry in the amount of color spreading from two inducing lines such that the color of the line with less luminance contrast relative to the background spreads proportionally more than the color of the line with more luminance contrast?

This happens in the BCS because the spatial competition is stronger from the boundaries of higher-contrast edges to those of lower-contrast edges than conversely. The boundaries of the lower-contrast edges are thus weakened more by competition than the boundaries of the higher-contrast edges. Hence more color can spread across these boundaries than conversely. A similar idea was used to explain why neon color spreading is sensitive to the relative contrasts of the edges at which neon color is released.<sup>3</sup>

A more recent model of how perceptual boundaries are formed within the laminar circuits of visual cortex clarifies how BCS operations are realized by identified cortical circuits. This LAMINART model proposes that spatial competition during boundary formation occurs between layers 6 and 4 of cortical areas V1 and V2.<sup>37–41</sup> The LAMINART model explains a much larger set of data than was possible with the original BCS, including anatomical and neurophysiological data that support all the model's proposed cell and circuit properties.

The existence of spatial competition does not imply that the lower-contrast boundaries are entirely suppressed. If they were, then the color of the lower-contrast edge could not be distinguished from the watercolor that it causes. A key property of competitive and cooperative boundary interactions in the BCS and subsequent LAMINART models is that they preserve their analog sensitivity in response to the intensity of the inputs that drive them. This property, which is called *analog coherence*, has been shown through computer simulations to be robustly realized by the laminar circuits that carry out boundary grouping in cortical areas V1 and V2.<sup>37–40</sup> This analog sensitivity depends on the fact that competition within the model uses on-center off-surround networks whose cells obey membrane equations with shunting dynamics, which lead to contrast normalization properties.<sup>42,43</sup> These contrast-sensitive properties were used in the original Grossberg and Mingolla<sup>3</sup> explanation of neon color spreading properties and have subsequently been used to explain other cortical data by many authors; e.g., Heeger<sup>44</sup> and Douglas *et al.*<sup>45</sup>

An implication of this competition hypothesis is that

any boundary that can produce a similar weakening of a nearby, less contrastive, boundary at a colored region of prescribed size can cause a similar amount of color spreading from that region. This property can explain the approximately equal chromatic effects in cases 1 through 6 in Fig. 11, despite the difference in the length of the purple and orange contours. The main effect is a local one whereby the more contrastive boundaries due to the purple regions inhibit the less contrastive boundaries due to the contiguous orange regions.

The watercolor illusion, as in Fig. 3 and 4, derives its strength from the fact that a more contrastive and less contrastive edge are parallel to each another over a significant spatial extent. Thus the total effect is derived from color leakage across the entire length of the weaker boundary, among others.

### C. Cooperative Boundary Groupings Contain Color Spreading

The competition effect is not sufficient to explain all aspects of neon color spreading and the watercolor effect. One basic additional property that must be explained is how the color that spreads from spatially discrete or continuous inducers can be contained within prescribed regions of space. For the watercolor illusion in Figs. 3 and 4, continuous boundaries exist whereby to contain the spreading color. For the neon color spreading and limiting cases of Figs. 10 and 11, there are no explicit boundaries within the images themselves. The brain creates these boundaries. This is achieved through a cooperative process whereby boundary groupings are formed and completed, as during the formation of illusory contours, and also through the manner in which cortical competitive and cooperative boundary and surface processes interact to generate 3D boundaries and surfaces that exhibit figure-ground separation effects.

Boundary completion, including illusory contour formation, was predicted by the BCS to depend on a long-range oriented cooperation process whereby boundaries could form across image locations that receive no bottom-up contrastive signals.<sup>2-4,34</sup> This cooperative process was predicted to obey a *bipole property* whereby the cooperating cells could fire, even if they received no direct bottom-up input, if they received (almost) colinear inputs with (almost) their preferred orientation from positions on both sides of their receptive field. Since these original predictions were made, neurophysiological, anatomical, and perceptual experiments have provided supportive evidence, and it has been possible to interpret both the competitive and the cooperative BCS mechanisms in terms of identified cells within the laminar circuits of cortical areas V1 and V2. Several recent articles review how this LAMINART model's cooperative and competitive feedforward and feedback mechanisms can be used to explain a large body of perceptual, anatomical, and neurophysiological data.<sup>37-41,46-50</sup>

For present purposes, the most important hypothesis is the following: The bipole property is predicted to be realized by cells in layer 2/3 of cortical area V2 that interact together via long-range horizontal connections (Figs. 12(b) and 12(c)). The spatial competition from layers 6 to 4 of V2 (Figs. 12(b) and 12(c)) directly influences the input

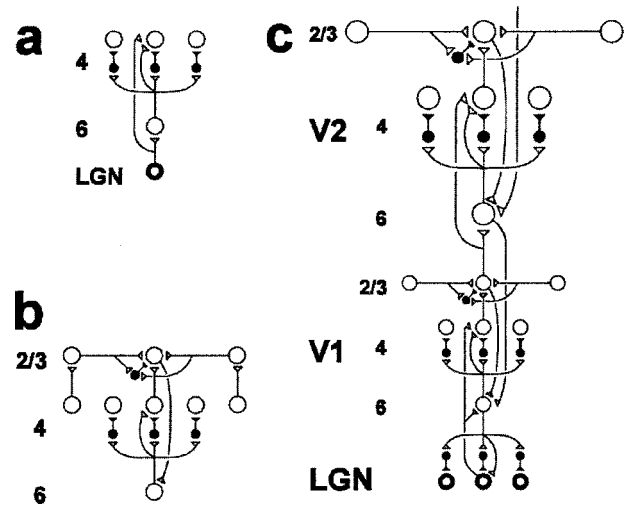


Fig. 12. Some known cortical connections that are joined together in the LAMINART model of bottom-up, horizontal, and top-down interactions within visual cortical areas V1 and V2. See Raizada and Grossberg<sup>40</sup> for summaries of supportive anatomical and neurophysiological data. Inhibitory interneurons are shown as filled-in black symbols. (a) The LGN provides bottom-up activation to layer 4 via two routes. First, it makes a strong connection directly into layer 4. Second, LGN axons send collaterals into layer 6 and thereby also activate layer 4 via the 6→4 on-center off-surround path. The combined effect of the bottom-up LGN pathways is to stimulate layer 4 via an on-center off-surround, which provides divisive contrast normalization of layer 4 cell responses. The excitatory and inhibitory layer 6 inputs to the layer 4 on-center are approximately balanced. As a result, the on-center receives a modulatory, but not driving, input. (b) Connecting the 6→4 on-center off-surround network to the layer 2/3 grouping circuit: Like-oriented layer 4 simple cells with opposite polarities compete (not shown) before generating half-wave rectified outputs that converge onto layer 2/3 complex cells in the column above them. Layer 2/3 contains long-range oriented recurrent connections to other layer 2/3 cells. A balance between excitation via long-range horizontal connections and short-range disinhibitory interneurons helps to control which layer 2/3 cells will fire, as does interlaminar feedback: Layer 2/3 cells send activation to enhance their own positions in layer 4 via the 6→4 on-center and to suppress input to other layer 2/3 cells via the 6→4 off-surround. There exist direct layer 2/3→6 connections in macaque V1, as well as indirect routes via layer 5. (c) V2 repeats the laminar pattern of V1 circuitry but at a larger spatial scale. In particular, perceptual groupings form using the V2 horizontal layer 2/3 connections, which have a longer range than the connections in layer 2/3 of V1. V1 layer 2/3 projects up to V2 layers 6 and 4, just as LGN projects to layers 6 and 4 of V1. Higher cortical areas send attentional feedback into V2, which ultimately reaches layer 6, just as V2 feedback acts on layer 6 of V1. Feedback paths from higher cortical areas straight into V1 (not shown) can complement and enhance feedback from V2 into V1. Top-down attention can also modulate layer 2/3 pyramidal cells directly by activating both the pyramidal cells and the inhibitory interneurons in that layer. The inhibition tends to balance the excitation, leading to a modulatory effect. These top-down attentional pathways tend to synapse on apical dendrites in layer 1, which are not shown, for simplicity. (Reprinted with permission from Grossberg and Raizada.<sup>39</sup>)

strengths from layer 4 that activate the long-range horizontal connections in layer 2/3 of V2 that form perceptual boundaries. When the spatial competition weakens the activities of layer 4 cells, the perceptual boundaries in layer 2/3 that would otherwise form in response to these layer 4 inputs are correspondingly weakened. These weakened boundaries generate weakened barriers to

filling-in within the filling-in domains of the surface cortical processing stream; e.g., the thin stripes of cortical area V2 and their projections to V4. As a result, discounted bottom-up color signals to these filling-in domains can spread, or fill in, more easily across these boundary positions.

As noted above, sensitivity to relative contrast had earlier been used to explain why neon color spreading is sensitive to the relative contrasts of the edges at which neon color is released.<sup>3</sup> Here too, interacting competitive and cooperative boundary grouping processes played a key role. The main idea was again that boundaries at positions of lower contrast are weakened more than spatially contiguous boundaries at positions of higher contrast, as at the orange lines that abut the more contrastive purple lines in Fig. 10. Another factor in the explanation of neon color spreading is the ability of the BCS to form illusory contours that are perpendicular (among other orientations) to the inducing lines that initiate spreading and to thereby contain the filling-in process within the square annular regions in Fig. 10.

The BCS predicted that these illusory contours are formed by the same cooperative-competitive interactions that weaken the boundaries through which neon color can spread.<sup>3</sup> The first step in forming these illusory contours is the generation of small boundaries, called *end cuts*, at line ends. These boundaries form owing to the way in which spatial competition interacts with competition between orientations at each position.<sup>3,32</sup> The end cuts at a line end are activations of a population of cells that have a range of orientational preferences that are perpendicular, or almost perpendicular, to that of the inducing line. Such a fuzzy range of end-cut orientational preferences derives from the way in which oriented complex cells interact with spatial and orientational competition mechanisms. The existence of this fuzzy range of orientations makes it more likely that grouping can be initiated among like-oriented end cuts that are collinear across position.

Like-oriented end cuts that are collinear across position use bipole cooperation to form illusory contours. In Fig. 10, these illusory contours are approximately perpendicular to the purple line ends and pass through the positions where the lines change color, thereby forming a square annular boundary that can contain the spreading orange color. These illusory contours can be quite sharp, despite the fuzziness of the end-cut orientations, because bipole cooperation interacts via feedback with spatial and orientational competition to inhibit weaker cell responses. This sharpening of end cuts during illusory contour formation is another example of hierarchical resolution of uncertainty. The initial fuzziness is needed to initiate boundary grouping but risks a loss of acuity. The ensuing sharpening by cooperative-competitive interactions permits the resulting grouping to form without a loss of acuity. Such boundary and surface interactions have elsewhere been used to explain a variety of additional data about neon color spreading.<sup>3,32,50-53</sup>

#### D. Why Assimilation is Weaker than Neon

This explanation also clarifies why the assimilation effects in cases 7 and 8 in Fig. 11 are weaker than the neon and watercolor illusion effects. Consider case 7 for a good

example of this phenomenon. The ends of the orange lines can create end cuts that can form a bounding illusory contour, again in the form of a square annular boundary. Here, too, the bipole cooperation interacts via feedback with the spatial and orientational competition. It can hereby weaken the boundaries at the ends of the orange lines a little but not nearly so much as the more contrastive purple boundaries. As a result, some color can spread into the square annulus. In case 8, the inducers are so short that they create very weak, if any, end cuts and a weak, if any, illusory contour. Any assimilation that can occur will be correspondingly weak.

#### E. Three-Dimensional Surfaces and Figure-Ground Separation in the Watercolor Illusion

Figures 3, 4, 7, and 8 illustrate the fact that the watercolor illusion can generate percepts of rounded 3D surfaces and can lead to figure-ground separated percepts of transparent surfaces lying above a background surface. FAÇADE theory proposes how 2D monocular properties of the BCS and FCS may be naturally embedded into a more comprehensive theory of 3D vision and figure-ground separation that was introduced in Grossberg<sup>31-33</sup> and further developed in a series of quantitative studies to explain and simulate several different types of perceptual and neural data.<sup>46,48,50,53-58</sup>

In particular, FAÇADE theory proposes how brain processes that have evolved in order to represent the world in three dimensions also enable us to perceive 2D images as figures and backgrounds in depth. Some of these figure-ground mechanisms permit partially overlapping, occluding, and occluded image parts to be separated and completed in depth. The same mechanisms shed light on how the watercolor illusion can support a figural percept. In Figs. 3 and 4, for example, the watercolor illusion segregates the colored frame in depth and gives it the appearance of a rounded figural surface. This rounded percept becomes stronger as the contrast ratio between the two colored lines is increased, as Fig. 9 illustrates.

Several factors contribute to these percepts within FAÇADE theory. One factor is that there are depth-specific and color-specific networks within the surface stream where filling-in occurs. These networks are called filling-in domains, or FIDOs. FAÇADE theory proposes how depth-specific boundaries can selectively capture color signals to fill in at one depth but not others. Surface filling-in within a particular FIDO is seen at a prescribed relative depth from the observer. This fact helps to explain how the achromatic and chromatic filled-in surfaces of a watercolor illusion get separated from each other, but it is not sufficient to explain which surface will appear as figure and which as ground.

The determination of figure and background can be traced to how boundaries interact with surface inducers to selectively fill in FIDOs that represent different depths. In particular, when two colored lines of different contrast are contiguous, as with the purple and orange lines in Figs. 3 and 4, then three parallel rows of boundaries are generated, usually of progressively decreasing boundary strength. Such an array generates a spatially sparse version of a *boundary web*, or spatial array of boundaries that can restrict filling-in within relatively

small surface regions. Earlier modeling studies predicted how a boundary web can elicit a percept of a rounded surface in depth.<sup>51,59</sup> This prediction was successfully tested in experiments using depth-from-texture images by Todd and Akerstrom.<sup>60</sup> In their data, the worst correlation between human psychophysical judgments of 3D shape from texture and model predictions was 0.985.

The main idea behind this predictive success can be summarized as follows, before it is applied to explain watercolor effect figural properties. Consider a 2D shaded ellipse. How does such a 2D image generate a percept of a 3D curved surface? The 2D image activates multiple filters, each sensitive to a different range of spatial scales (see the bottom-up pathways to layer 4 in Figs. 12(b) and 12(c)). Other things being equal, larger filters need bigger inputs to fire than do smaller filters. Likewise, larger filters can, other things being equal, binocularly fuse more binocularly disparate images, representing closer objects, than can smaller filters. Smaller filters can binocularly fuse only less binocularly disparate images and thus farther objects. In addition, larger filters can respond to a wider range of disparities than can smaller filters. As a result, an object at a given depth with respect to an observer can initially be represented by multiple spatial scales. These disparity-selective properties of multiple-scale filters often go under the name of the size-disparity correlation.<sup>61–68</sup>

How does the brain decide which combination of multiple-scale filters will ultimately represent the depth of an object? The multiple-scale filters input to grouping cells, via layer 4-to-2/3 connections in cortical area V2, which use the same cooperative-competitive interactions that have already been mentioned to select and complete boundary representations that are sensitive to different depths. These competitive interactions include the spatial competition that helps to explain how the watercolor effect occurs. Then, as already mentioned, the winning depth-selective boundaries selectively capture color inputs at FIDOs that fill in the captured color at the corresponding depth, while also bounding the regions within the color can spread. If some of these boundaries are weakened, as in the contrast-sensitive spatial competition described above, then color can flow out of a region to the extent that the boundary has been weakened.

Now consider how multiple scales may respond to a shaded ellipse. Other things being equal, smaller scales can fire more easily nearer to the bounding edge of the ellipse. As the spatial gradient of shading becomes more gradual with distance from the bounding edge, it becomes harder for smaller scales to respond to this gradient. Thus, other things being equal, larger scales tend to respond more as the distance from the bounding edge increases. As a result, the regions nearer to the center of the ellipse look closer owing to the size-disparity correlation.

A similar thing happens, albeit with a more spatially discrete filter input, in response to a watercolor image such as the ones in Figs. 4 and 5. Here, just as in response to a shaded ellipse, there is a spatial array of successively weaker filter responses as the distance increases from the most contrastive edge of the display. These successively weaker filter responses activate boundary and surface processes much as one would expect from a spatially dis-

crete version of a shaded ellipse, and these processes can generate a rounded appearance using the same size-disparity correlation mechanisms. A new property of the watercolor effect, which is due to the discrete changes in successive boundary contrasts, is that the spatially disjoint boundaries can weaken each other via spatial competition and thereby allow surface color to spread within the depth-selective boundaries that are formed in response to the multiple-scale filter responses. That is why the interior of the watercolor region can look a little closer to the observer than the bounding edge. Because of this perceived depth difference, a region suffused with the watercolor illusion can have a stronger figural quality than one filled with a uniform color, which tends to look flat.

## F. Transparency in the Watercolor Illusion

Figure 8 illustrates how the watercolor effect can create transparent percepts. In this figure, the contrast of the watercolor bounding contour is greater than that of the vertical boundary, thereby creating a stronger boundary around the watercolor region. This property is enough to initiate a figure-ground separation process whereby the watercolor boundary can be seen in front of the vertical boundary. See Grossberg and Yazdanbakhsh<sup>50</sup> or Kelly and Grossberg<sup>57</sup> for an explanation of how this happens. Because the conditions for the watercolor illusion are also present—namely, the parallel purple and orange lines—these nearer boundaries can fill in yellowish surface color owing to the spatial competition among the watercolor boundaries that was described above. The two gray surfaces can also fill in at the same positions but on a FIDO that represents a slightly farther depth plane. Hence, a transparent surface percept is seen.

## ACKNOWLEDGMENTS

B. Pinna was supported by Fondazione Banco di Sardegna, the Alexander von Humboldt Foundation, ERSU, Banca di Sassari and Fondo d'Ateneo (ex 60%). S. Grossberg was supported in part by the National Science Foundation (NSF SBE-0354378) and the Office of Naval Research (ONR N00014-01-1-0624). We thank Massimo Dasara for assistance in testing the subjects.

Corresponding author Stephen Grossberg can be reached by e-mail at [steve@bu.edu](mailto:steve@bu.edu).

## REFERENCES

1. L. G. Thorell, L. G. De Valois, and D. G. Albrecht, "Spatial mapping of monkey V1 cells with pure color and luminance stimuli," *Vision Res.* **24**, 751–769 (1984).
2. M. Cohen and S. Grossberg, "Neural dynamics of brightness perception: features, boundaries, diffusion, and resonance," *Percept. Psychophys.* **36**, 428–456 (1984).
3. S. Grossberg and E. Mingolla, "Neural dynamics of form perception. Boundary completion, illusory figures and neon color spreading," *Psychol. Rev.* **92**, 173–211 (1985).
4. S. Grossberg and E. Mingolla, "Neural dynamics of perceptual grouping: textures, boundaries, and emergent segmentations," *Percept. Psychophys.* **38**, 141–171 (1985).
5. D. Varin, "Fenomeni di contrasto e diffusione cromatica nell'organizzazione spaziale del campo percettivo," *Riv. di Psicol.* **65**, 101–128 (1971).

6. P. Bressan, E. Mingolla, L. Spillmann, and T. Watanabe, "Neon colour spreading: a review," *Perception* **26**, 1353–1366 (1997).
7. H. F. J. M. van Tuijl, "A new visual illusion: neon-like color spreading and complementary color induction between subjective contours," *Acta Psychol.* **39**, 441–445 (1975).
8. H. F. J. M. van Tuijl and C. M. M. de Weert, "Sensory conditions for the occurrence of the neon spreading illusion," *Perception* **8**, 211–215 (1979).
9. D. Katz, "Die Erscheinungsweisen der Farben und ihre Beeinflussung durch die individuelle Erfahrung," *Z. Psychol., Ergänzungsbd* **7**, 6–31 (1911).
10. D. Katz, *Die Erscheinungsweisen der Farben*, 2nd ed (1930) [translation into English: R. B. MacLeod and C. W. Fox, *The World of Color* (Kegan Paul, 1935)].
11. P. Bressan, "Revisitation of the luminance conditions for the occurrence of the achromatic neon color spreading illusion," *Percept. Psychophys.* **54**, 55–64 (1993).
12. K. Koffka, *Principles of Gestalt Psychology* (Harcourt, Brace, 1935).
13. W. Metzger, *Psychologie, Die Entwicklung ihrer Grundannahmen seit der Einführung des Experimentes*, Zweite Auflage (Steinkopff, Darmstadt, 1954).
14. F. Devinck, P. B. Delahunt, J. L. Hardy, L. Spillmann, and J. S. Werner, "The watercolor effect: quantitative evidence for luminance-dependent mechanisms in long-range color assimilation," *Vision Res.* **45**, 1413–1424 (2005).
15. B. Pinna, "Un effetto di colorazione," in *Il laboratorio e la città. XXI Congresso degli Psicologi Italiani*, V. Majer, M. Maeran, and M. Santinello, eds. Edizioni SIPs, Società Italiana di Psicologia, Milano, 1987), p. 158.
16. B. Pinna, G. Brelstaff, and L. Spillmann, "Surface color from boundaries: a new 'watercolor' illusion," *Vision Res.* **41**, 2669–2676 (2001).
17. B. Pinna, J. S. Werner, and L. Spillmann, "The watercolor effect: a new principle of grouping and figure-ground organization" *Vision Res.* **43**, 43–52 (2003).
18. L. Spillmann, B. Pinna, and J. S. Werner, "Form-from-watercolour in perception and old maps," in *Seeing Spatial Form*, M. R. M. Jenkin and L. R. Harris, eds. (Oxford U. Press) (to be published).
19. B. Pinna, "The role of Gestalt principle of similarity in the watercolour illusion," *Spatial Vis.* **21**, 1–8 (2005).
20. C. von Campenhausen and J. Schramme, "100 years of Benham's top in colour science," *Perception* **24**, 695–717 (1995).
21. B. Pinna, "The neon color spreading and the watercolor illusion: phenomenal links and neural mechanisms," in *Variety of Complex Systems Behaviors, Proceedings of the Third National Conference on Systems Science*, G. Minati and E. Pessa, eds. (Kluwer Academic, 2005).
22. M. Wertheimer, "Untersuchungen zur Lehre von der Gestalt II," *Psychol. Forsch.* **4**, 301–350 (1923).
23. E. Rubin, *Synsoplevede Figurer* (Gyldendalske, 1915).
24. E. Rubin, *Visuell wahrgenommene Figuren* (Gyldendalske Boghandel, 1921).
25. C. Redies and L. Spillmann, "The neon color effect in the Ehrenstein illusion," *Perception* **10**, 667–681 (1981).
26. P. Bressan, "Neon color spreading with and without its figural prerequisites," *Perception* **22**, 353–361 (1993).
27. J. M. Kennedy, "Illusory contours and the ends of lines," *Perception* **7**, 605–607 (1978).
28. M. Sabin, "A dynamic model of anomalous figures," in *The Perception of Illusory Contours*, S. Petry and G. E. Meyer, eds. (Springer, New York, 1987), pp 131–142.
29. T. F. Shipley and P. J. Kellman, "The role of discontinuities in the perception of subjective figures," *Percept. Psychophys.* **48**, 259–270 (1990).
30. C. Redies, L. Spillmann, and K. Kunz, "Colored neon flanks and line gap enhancement," *Vision Res.* **24**, 1301–1309 (1984).
31. S. Grossberg, "Cortical dynamics of three-dimensional form, color, and brightness perception: II: Binocular theory," *Percept. Psychophys.* **41**, 117–158 (1987).
32. S. Grossberg, "3-D vision and figure-ground separation by visual cortex," *Percept. Psychophys.* **55**, 48–120 (1994).
33. S. Grossberg, "Cortical dynamics of three-dimensional figure-ground perception of two-dimensional pictures," *Psychol. Rev.* **104**, 618–658 (1997).
34. S. Grossberg, "Outline of a theory of brightness, color, and form perception," in *Trends in Mathematical Psychology*, E. Degreef and J. van Buggenhaut, eds. (North-Holland, 1984), pp. 59–86.
35. S. Grossberg and D. Todorovic, "Neural dynamics of 1-D and 2-D brightness perception: a unified model of classical and recent phenomena," *Percept. Psychophys.* **43**, 241–277 (1988).
36. S. Grossberg, "The complementary brain: unifying brain dynamics and modularity," *Trends in Cogn. Sci.* **4**, 233–245 (2000).
37. S. Grossberg, "How does the cerebral cortex work? Learning, attention and grouping by the laminar circuits of visual cortex," *Spatial Vis.* **12**, 163–186 (1999).
38. S. Grossberg, E. Mingolla, and W. D. Ross, "Visual brain and visual perception: How does the cortex do perceptual grouping?" *Trends Neurosci.* **20**, 106–111 (1997).
39. S. Grossberg and R. D. S. Raizada, "Contrast-sensitive perceptual grouping and object-based attention in the laminar circuits of primary visual cortex," *Vision Res.* **40**, 1413–1432 (2000).
40. R. D. S. Raizada, and S. Grossberg, "Context-sensitive binding by the laminar circuits of V1 and V2: a unified model of perceptual grouping, attention, and orientation contrast," *Special Issue on Neural Binding of Space and Time, Visual Cogn.* **8** (3/4/5), 431–466 (2001).
41. R. D. S. Raizada and S. Grossberg, "Towards a theory of the laminar architecture of cerebral cortex: computational clues from the visual system," *Cereb. Cortex* **13**, 100–113 (2003).
42. S. Grossberg, "Contour enhancement, short term memory, and constancies in reverberating neural networks," *Stud. Appl. Math.* **52**, 217–257 (1973). Reprinted in S. Grossberg, *Studies of Mind and Brain* (Reidel, 1982).
43. S. Grossberg, "How does a brain build a cognitive code?" *Psychol. Rev.* **87**, 1–51 (1980).
44. D. J. Heeger, "Normalization of cell responses in cat striate cortex," *Visual Neurosci.* **9**, 181–197 (1992).
45. R. J. Douglas, C. Koch, M. Mahowald, K. A. C. Martin, and H. H. Suarez, "Recurrent excitation in neocortical circuits," *Science* **269**, 981–985 (1995).
46. Y. Cao and S. Grossberg, "A laminar cortical model of stereopsis and 3D surface perception: closure and da Vinci stereopsis," *Techn. Rep. CAS/CNS-TR-2004-007. Spatial Vis.* (to be published).
47. S. Grossberg, "How does the cerebral cortex work? Development, learning, attention, and 3D vision by laminar circuits of visual cortex," *Behav. Cog. Neurosci. Rev.* **2**, 47–76 (2003).
48. S. Grossberg and P. A. Howe, "Laminar cortical model of stereopsis and three-dimensional surface perception," *Vision Res.* **43**, 801–829 (2003).
49. S. Grossberg and J. R. Williamson, "A neural model of how horizontal and interlaminar connections of visual cortex develop into adult circuits that carry out perceptual grouping and learning," *Cereb. Cortex* **11**, 37–58 (2001).
50. S. Grossberg and A. Yazdanbakhsh, "Laminar cortical dynamics of 3D surface perception: stratification, transparency, and neon color spreading," *Vision Res.* **45**, 1725–1743 (2005).
51. S. Grossberg, "Cortical dynamics of three-dimensional form, color, and brightness perception, I: Monocular theory," *Percept. Psychophys.* **41**, 87–116 (1987).
52. S. Grossberg, "A comment on 'Assimilation of achromatic color cannot explain the brightness effect in the achromatic neon effect' by M. K. Albert," *Perception* **28**, 1291–1302 (1999).
53. S. Grossberg and G. Swaminathan, "A laminar cortical model for 3D perception of slanted and curved surfaces and of 2D images: development, attention, and bistability," *Vision Res.* **44**, 1147–1187 (2004).

54. S. Grossberg and F. Kelly, "Neural dynamics of binocular brightness perception," *Vision Res.* **39**, 3796–3816 (1999).
55. S. Grossberg and N. P. McLoughlin, "Cortical dynamics of three-dimensional surface perception: binocular and half-occluded scenic images," *Neural Networks* **10**, 1583–1605 (1997).
56. S. Grossberg and L. Pessoa, "Texture segregation, surface representation and figure-ground separation," *Vision Res.* **38**, 1657–1684 (1998).
57. F. Kelly and S. Grossberg, "Neural dynamics of 3-D surface perception: figure-ground separation and lightness perception," *Percept. Psychophys.* **62**, 1596–1618 (2000).
58. N. P. McLoughlin and S. Grossberg, "Cortical computation of stereo disparity," *Vision Res.* **38**, 91–99 (1998).
59. S. Grossberg and E. Mingolla, "Neural dynamics of surface perception: boundary webs, illuminants, and shape-from-shading," *Comput. Vis. Graph. Image Process.* **37**, 116–165 (1987).
60. J. T. Todd and R. A. Akerstrom, "Perception of three-dimensional form from patterns of optical texture," *J. Exp. Psychol. Hum. Percept. Perform.* **13**, 242–255 (1987).
61. B. Julesz and R. A. Schumer, "Early visual perception," *Annu. Rev. Psychol.* **32**, 575–627 (1981).
62. J. J. Kulikowski, "Limit of single vision in stereopsis depends on contour sharpness," *Nature* **275**, 126–127 (1978).
63. W. A. Richards and M. G. Kaye, "Local versus global stereopsis: two mechanisms?" *Vision Res.* **14**, 1345–1347 (1974).
64. C. M. Schor and C. W. Tyler, "Spatio-temporal properties of Panam's fusional area," *Vision Res.* **21**, 683–692 (1981).
65. C. M. Schor and I. Wood, "Disparity range for local stereopsis as a function of luminance spatial frequency," *Vision Res.* **23**, 1649–1654 (1983).
66. C. M. Schor, I. Wood, and J. Ogawa, "Binocular sensory fusion is limited by spatial resolution," *Vision Res.* **24**, 661–665 (1984).
67. C. W. Tyler, "Spatial organization of binocular disparity sensitivity," *Vision Res.* **15**, 583–590 (1975).
68. C. W. Tyler, "Sensory processing of binocular disparity," in *Basic and Clinical Aspects of Binocular Vergence Eye Movements*, Schor and Ciuffreda, eds. (Butterworths, 1983), pp. 199–295.